*Journal of Structural Geology*, Vol. 5, No. 3/4, pp. 245 to 253, 1983
Printed in Great Britain

0191-8141/83 $3.00+0.00
Pergamon Press

# Finite strain determination of gneiss: application of Fry's method to porphyroid in the southern Massif Central (France)

ROBIN LACASSIN and JEAN VAN DEN DRIESSCHE

Laboratoire de Géologie Structurale, LA 266, C.N.R.S., U.S.T.L., 34060 Montpellier Cédex, France

(*Received* 2 *April* 1982; *accepted in revised form* 19 *November* 1982)

**Abstract**—We present an attempt to apply Fry's method of finite strain ellipsoid determination to deformed gneissic rocks. Several finite strain ellipsoids have been measured on different 'porphyroid' gneiss samples from the Cévennes area (Southern Massif Central, France). The ellipsoids are characterized by a $K$ parameter close to 1 (plane strain) or $K > 1$ (constriction field). The method appears to be powerful, and we show that in some cases effects of a pretectonic fabric can be eliminated. From these results and microstructural data, a strain-path can be inferred.

**Résumé**—Nous essayons d'appliquer la méthode de détermination de l'ellipsoïde de déformation finie présentée par Fry, à des gneiss fortement déformés. Plusieurs ellipsoïdes de déformation finie ont été mesurés sur des échantillons de gneiss porphyroïdes provenant des Cévennes (Sud du Massif Central, France). Ces ellipsoïdes sont caractérisés par un paramètre $K$ proche de 1 (déformation plane) ou $K > 1$ (champ de la constriction).

La méthode est parfaitement utilisable dans ce type de roches, nous montrons par ailleurs que dans certains cas l'effet d'une fabrique prétectonique peut être éliminé. Nous déduisons un strain path de ces mesures de la déformation finie et de données microstructurales.

## INTRODUCTION

CLASSICALLY, the finite strain of rocks is measured on deformed markers such as fossils, ooliths, pebbles and reduction spots (e.g. Cloos 1947, Ramsay 1967, 1976). As strain markers are lacking in deep-level tectonites, there are only a few strain estimates in highly deformed and metamorphosed areas. Nevertheless it is an important parameter for understanding the tectonic history.

Most gneissic rocks show some recognizable pretectonic objects (individual crystals or grains); but the finite strain obtained from classical analysis of their eventual shape fabric generally underestimates the bulk strain and should be used carefully. The whole sample shape fabric (an $L$, $LS$ or $S$ tectonite) and the pressure-shadow crystallization (Choukroune 1971) give only a qualitative estimate of the ellipsoïd shape (i.e. oblate, plane strain or prolate, Flinn 1962, 1965).

Fry (1979) published a method of strain measurement based upon the relationships (distances) between the different objects in a rock. The present paper (1) tries to test this method in gneissic rocks, (2) provides finite strain results on a series of the Cevennes porphyroïdes gneisses (French Massif Central) and (3) discusses the regional and dynamical implications.

## THE METHOD

The deformation of a sample composed of objects in a matrix (with any relative rheological behaviour), is modelled by the deformation of a homogeneous matrix with embedded passive markers which correspond to the objects. In many cases, the relationships between the points (the centres of the 'object markers') constitute good strain markers (Fry 1979, Hanna & Fry 1979).

Fry considered the general case where the point distribution is related to a probability law, with a minimum interval set between the points. In an undeformed sample this minimum interval is assumed to be the same in any direction; in the deformed sample, it will be a function of the orientation of the straight line joining the two points considered. In the $XY$ plane this interval will be maximum when the line parallels $X$ and at its minimum when it parallels $Y$ (in the $YZ$ plane, respectively $Y$ and $Z$). $X > Y > Z$ are the strain ellipsoid axes. The ratios of these minimum and maximum distances are close to the finite strain ellipsoid axes ratios $X/Y$ and $Y/Z$. The finite strain determination is thus possible in rocks including undeformed objects: the measured finite strain is representative of the whole rock deformation.

To be usable, markers must satisfy the following conditions.

(1) In the undeformed stage, their distribution must not be altered by any anisotropy (e.g. sedimentary).
(2) In the deformed stage, the distribution should not be affected by a clastic behaviour.
(3) The minimum distance must be precisely defined by a high density of points.
(4) The markers should not interact.

## GEOLOGICAL SETTING

The French Massif-Central is mainly composed of metamorphic Palaeozoic and Precambrian rocks. The major Variscan tectonic features show a vergence to the south. The studied area is situated below the large thrust nappes described by Burg & Matte (1978). It is formed by a thick quartzo-pelitic sequence (Cambro-Ordovician) at the top of which the studied porphyroid gneisses are structurally intercalated (Shuaib 1952, Brouder 1963, Roger 1969, Pellet 1972).

*Description of the Cévennes porphyroid gneisses*

The gneiss matrix is quartzo-feldspathic with 10–30% biotite, muscovite and chlorite. The biotite commonly forms elongate spots (few cm) on the cleavage. The polycrystalline aggregates consist of plagioclase (An. 10–20) and some quartz, and constitute 20–30% of the rock. The aggregates vary in length from 1 to 10 cm. 'Blue quartz' coloured by rutile, typical of high temperature crystallization, has crystals 1 mm–1 cm and makes up 5–10% of the rock.

*The major deformation in the gneissic rocks*

The main deformation produced a penetrative composite cleavage, $S_{1\text{-}2}$, roughly horizontal and parallel to the stratification $S_0$ in the slates. The rock has a $LS$ tectonite shape fabric (Turner & Weiss 1963, Flinn 1962, 1965) (Fig. 1). A prominent stretching and mineral lineation is defined by the long axis of the plagioclase and biotite aggregates and by the alignment of micas. The average trend of this lineation $L_1$ is N0 40°, with slight variations (± 20°) (Fig. 3); it is subhorizontal in the cleavage plane (pitch < 20°). On the whole Massif Central scale, $L_1$ is subperpendicular to the cartographic trace of the main thrusts (Burg & Matte 1978).

A crenulation lineation, $L_{C1}$, superimposed on $L_1$, is often observed. These two lineations are generally parallel (Fig. 3). Locally this lineation, $L_{C1}$, is folded by later crenulations with various orientations (no measurement has been carried out in such specimens).

In the rock, the blue-quartz and the plagioclasic aggregates present characteristics of pretectonic objects (Fig. 2): they show evidence of internal strain (undulose extinction, sutured boundaries), fractures filled with equigranular quartz, pressure shadows occur around them and the cleavage is deflected in the matrix. Their deformation is generally weak (Fig. 2). An analysis of their shape fabric gives low shape ratios (Fig. 4). The contrasting rheological behaviour of matrix and markers may explain the discrepancy between the quartz shape ratios and the measurements with Fry's method. Nevertheless some accordance appears for the strain ellipsoid shape: the two calculated $K$ parameters (Flinn 1962) are close together.

*Quartz c-axis analysis*

We measured the c-axes of quartz in polycrystalline ribbons using a Universal Stage. Grains are small (50 $\mu$m) and isodiametric, showing an undulose extinction; they have sutured boundaries. These characters allow us to consider that plasticity mechanisms have been prominent in the quartz deformation. Deformation conditions of 300°C < T < 400°C and 3 < P < 5 kb are inferred from petrographic studies (Roger 1969, Pellet 1972) by persistence of blue quartz colouration and low crystallinity of biotites. According to these conditions, the principal slip system is (0001) ⟨a⟩ (Tullis *et al.* 1973, Blacic 1975, Nicolas & Poirier 1976, White 1976). Classical models (Etchecopar 1977, Bouchez 1978) may not explain the obtained fabric diagrams (Fig. 5).

The skeleton shapes (small circles centred on the stretching lineation) are similar to those presented by Burg (1981), who interpreted them, after Lister *et al.* (1978) and Lister & Hobbs (1980), as the results of a constrictional deformation.

## THE MARKERS USED IN THE PORPHYROID GNEISSES: METHODOLOGICAL IMPLICATIONS

For the finite strain analysis with Fry's method, two types of markers seem to be usable: the polycrystalline aggregates and the blue-quartz.

The origin of these gneisses is controversial (see above). We cannot exclude a pretectonic shape fabric of the aggregates or determine their centres precisely, so we did not use these objects. On the other hand, the blue-quartz satisfies these conditions. In most samples the density of quartz loci is high; thus the minimum distance is well defined. The blue-quartz, except broken crystals which we eliminated, are statistically isodiametric. Their diameter is lower or equal to the smallest dimension of the polycrystalline aggregates. If the rock is affected by a pretectonic fabric, according to the following model, their distribution remains isotropic.

More generally, we may model a rock in two dimensions by an assemblage of elliptical and circular passive markers in a matrix before deformation (Fig. 6a). After deformation (Fig. 6b) no more markers remain circular. Using a simple model, we show in Fig. 7 that it is possible to measure the tectonic strain, if, before deformation, the diameter of circular markers is equal to or lower than the smallest axis of the elliptical ones. This may be the case for a rock with a sedimentary shape fabric, composed of object with various initial shapes (some of them being spherical).

On the Fry's plot (Figs. 7 and 8) the strain ellipse is determined only for the models 1 and 3 (Fig. 7).

## RESULTS

Measurements have been carried out on sample surfaces parallel to the finite strain axes, assuming that the principal axes of the fabric of the rock coincide with those of the finite strain ellipsoid; that is $S_{1\text{-}2}$ is parallel to the $XY$ plane and $L_1$ parallel to $X$ ($X > Y > Z$) (Flinn 1965). The points (centres of the objects), located on sample surfaces, are digitized. The cut-off ellipse is traced by a high density of points, on the calculated Fry plot. The ellipse axes and estimated errors are directly measured on the plot. The obtained ellipse axes are always parallel to the macroscopic fabric axes ($S_{1\text{-}2}$, $L_1$).

On $XZ$ planes, we have obtained little results. Because the ellipse is highly elongate in this plane, and many clasts of blue-quartz can appear, it is difficult to determine precisely the ellipse ratio; and a great number

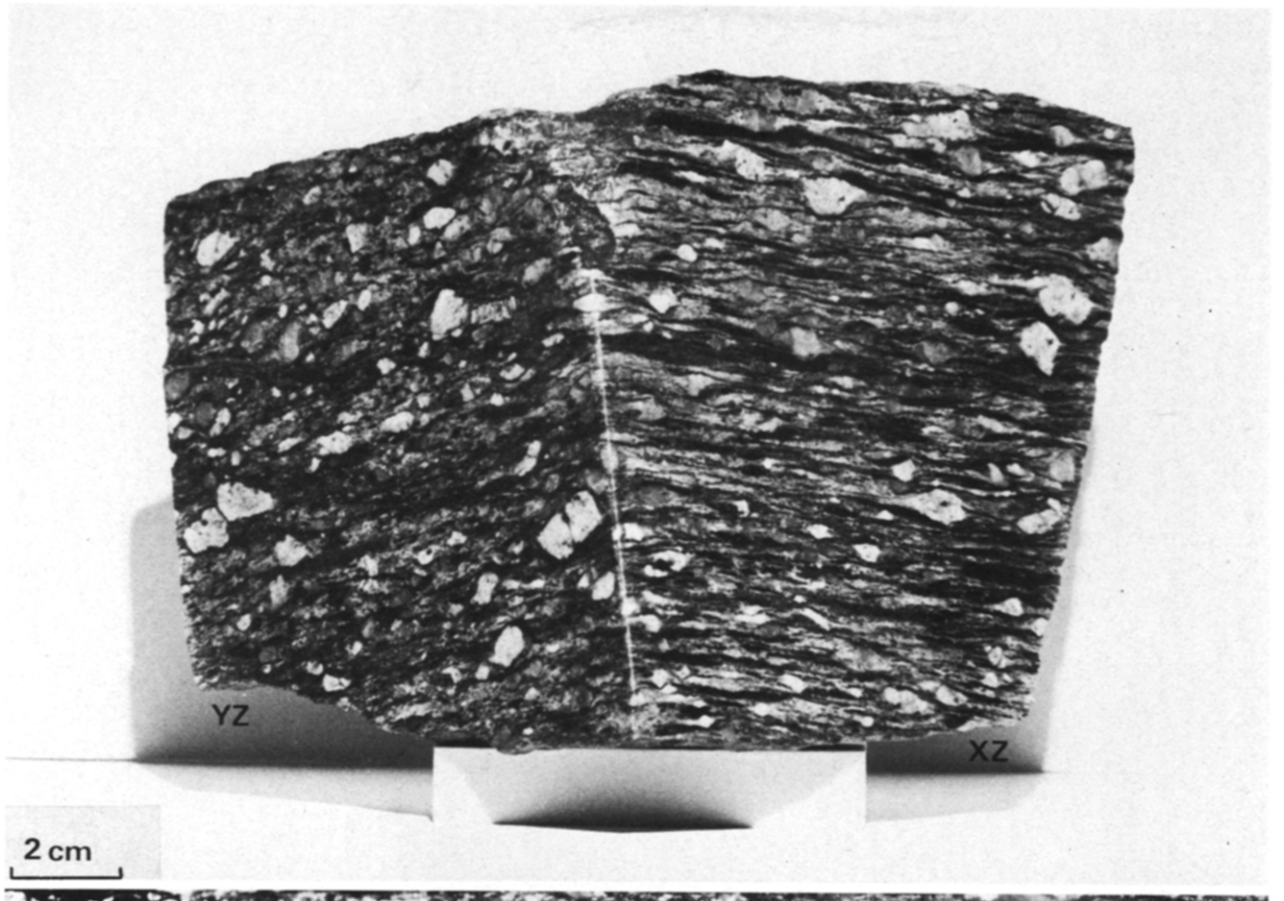


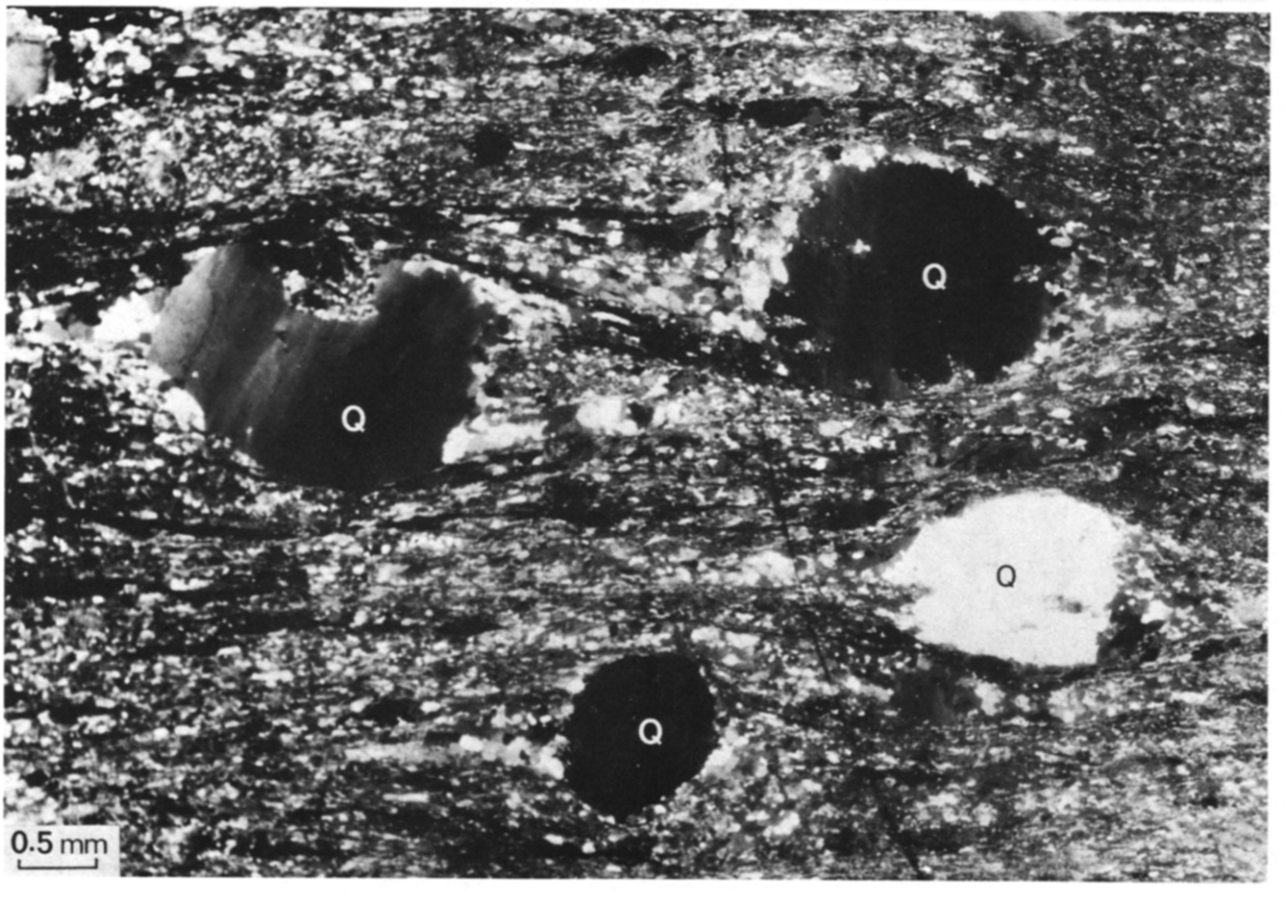


Fig. 1. Sample of porphyroid gneisses; faces parallel to the $XZ$ and $YZ$ planes.

Fig. 2. Photomicrograph under half crossed nicols ($XZ$ section); Q = blue quartz.

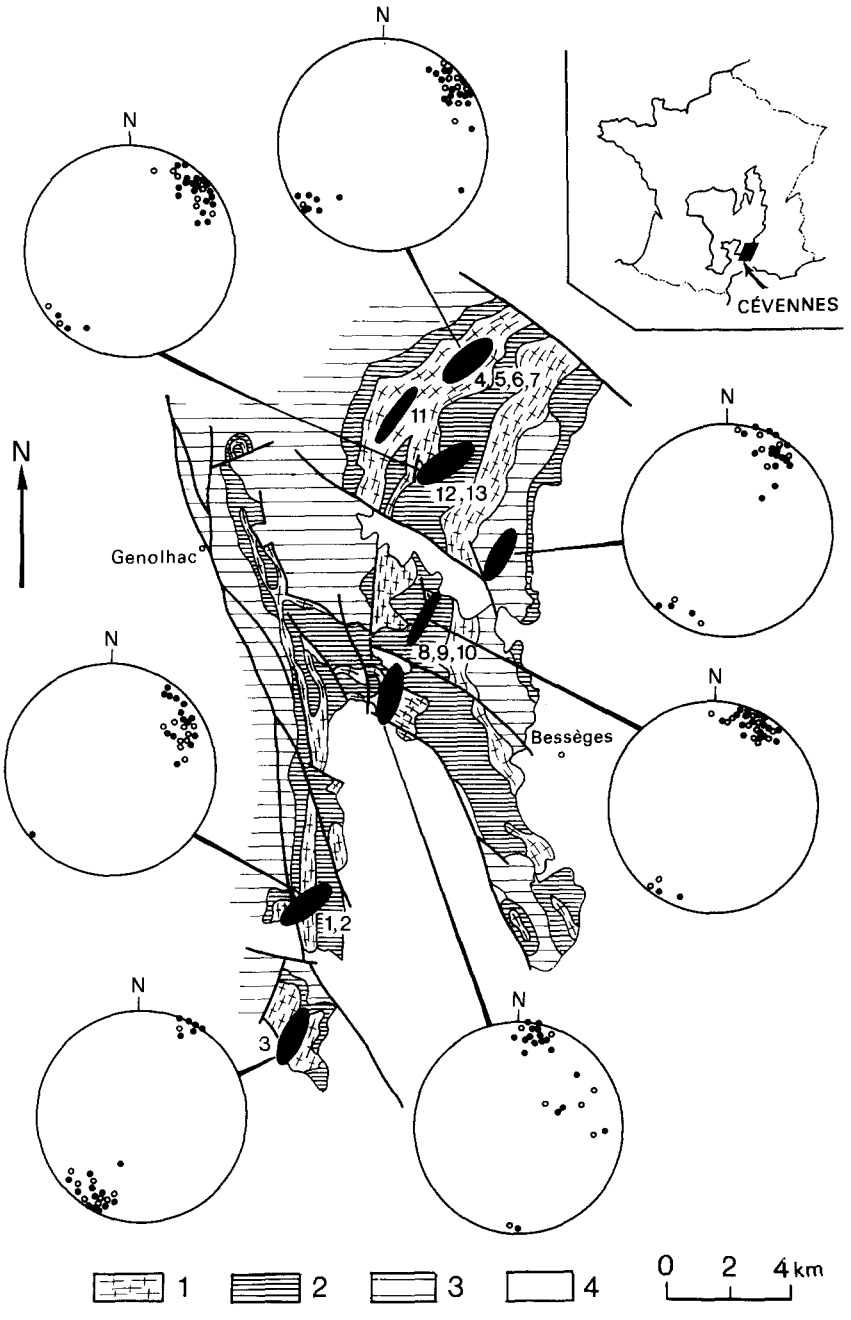


Fig. 3. Synthetic lineation map: 1, Porphyroid gneiss; 2, fine grained gneisses; 3, micaschists; 4, post-Hercynian cover. The black ellipses represent the trends of $L_{S1}$, their shapes represent the average ratios of the finite strain ellipses in the $XY$ plane. Numbers = sample localities. The black dots represent $L_1$ and the open circles represent the corrugation lineation ($L_{C1}$). (Lower hemisphere Schmidt nets.)

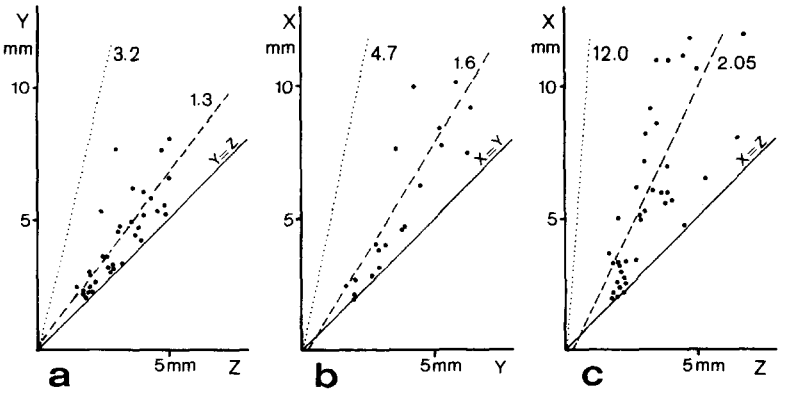


Fig. 4. Shape fabric of blue-quartz (sample 11). (a) $YZ$ section, (b) $XY$ section, (c) $XZ$ section. The dashed line represent the best fit line of linear correlation: $X/Y = 1.3$ (c = 0.8); $X/Y = 1.6$ (c = 0.85); $X/Z = 2.05$ (c = 0.8); (o < c < 1 = goodness of linear correlation, perfect when c = 1). The dotted line represent the measured strain ellipse axes ratio (Fry's method; Flinn shape parameter $K = 1.6$).

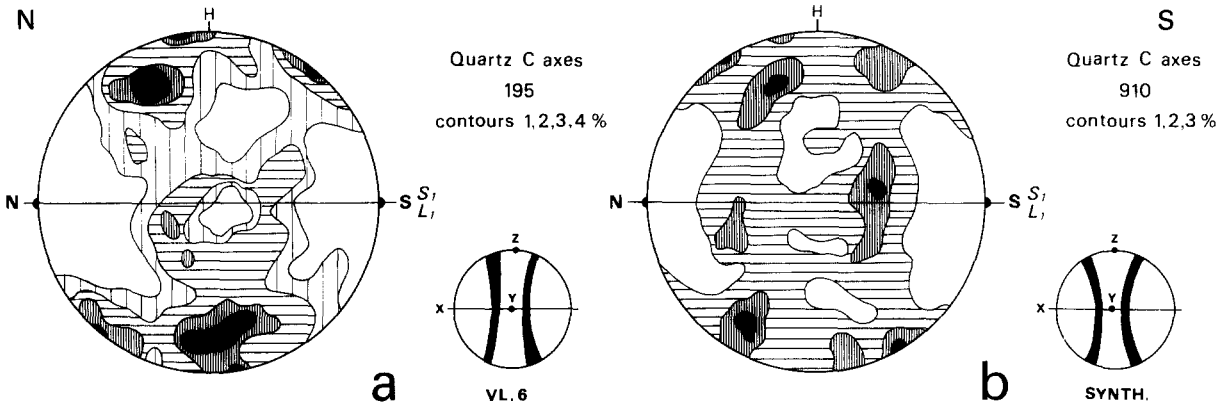


Fig. 5. Quartz preferred lattice orientation in $XZ$ sections (Schmidt nets, lower hemisphere). (a) sample 8 (195 c axes), contours: 1, 2, 3, 4% per 1% area, skeletal outline. (b) Synthetic fabric on three samples (910 c axes), contours: 1, 2, 3% per 1% area, skeletal outline.

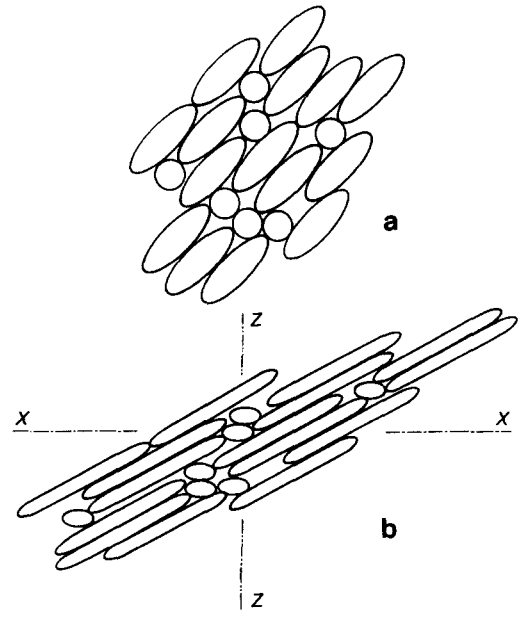


Fig. 6. Model with circular and elliptical objects, to simulate an initial sedimentary fabric: (a) non deformed, (b) deformed; $X$ and $Z$ are the finite strain axes.

of markers are necessary for a good definition (300–400 points). The defined ellipses have a maximum axial ratio of 12. On $XY$ and $YZ$ planes, about 100 objects are sufficient to obtain good ellipses.

The results for the different samples are in Table 1 and the corresponding strain parameter (Flinn 1962, 1965) determined. On a Flinn diagram (Fig. 9) each point is near the line $K = 1$ (plane strain); however, those corresponding to the most intensive deformation tend to be slightly constrictional ($K > 1$).

## DISCUSSION

### *Significance of the results*

The parallelism between the ellipse axes on Fry's plot and the macroscopic deformation axes supports the hypothesis of an initial isotropic distribution of the blue-quartz. According to the high goodness of the ellipse and the exceptional occurrence of crystals in contact (corresponding to rare points in the ellipse on Fry's plot), no prominent interaction should have occurred between the markers. So, the minimum distance was not originally defined by the impossibility of overlap of adjacent objects, but by the crystallization parameters of blue-quartz in volcanic rocks; these objects were dispersed in the matrix. In a compact assemblage of deformable objects (e.g. ooids), as stated by Fry (1979), the cut-off ellipse is correlated with the shape of the objects. In our case of weakly deformable objects dispersed in a matrix, the ellipse will represent the total finite strain undergone by the whole rock.

### *Interpretation*

Mattauer & Etchecopar (1976) interpreted the deformation of the Cevennes gneisses as a simple-shear regime, evidence provided by: (1) the presence of a subhorizontal cleavage; (2) a stretching and mineral lineation with a constant trend and (3) the shape fabric of gneissic rocks. The finite strain estimates (plane strain) with Fry's method, is not inconsistent with such a hypothesis.

The quartz fabrics may be interpreted (after Lister & Price 1978, Lister & Williams 1979, Brunel 1980) as the result of the great influence of the latest deformation increments.

The occurrence of a crenulation- (more exactly a corrugation) lineation parallel to the stretching lineation, when it is not related to an obvious late deformation seems to be general in a shear context associated with plane strain (e.g. Laurent & Etchecopar 1976 and personal communication, Hanmer 1979, Hugon & Le Corre 1979, Gratier & Vialon 1980, Steck 1980, Henderson 1981). However the mechanism of its formation is not well understood (Brun & Choukroune 1981).

Since all the samples arise from the same initial material, and according to the quartz fabrics and the occurrence of a late corrugation superimposed on the stretching lineation, we propose that a continous line

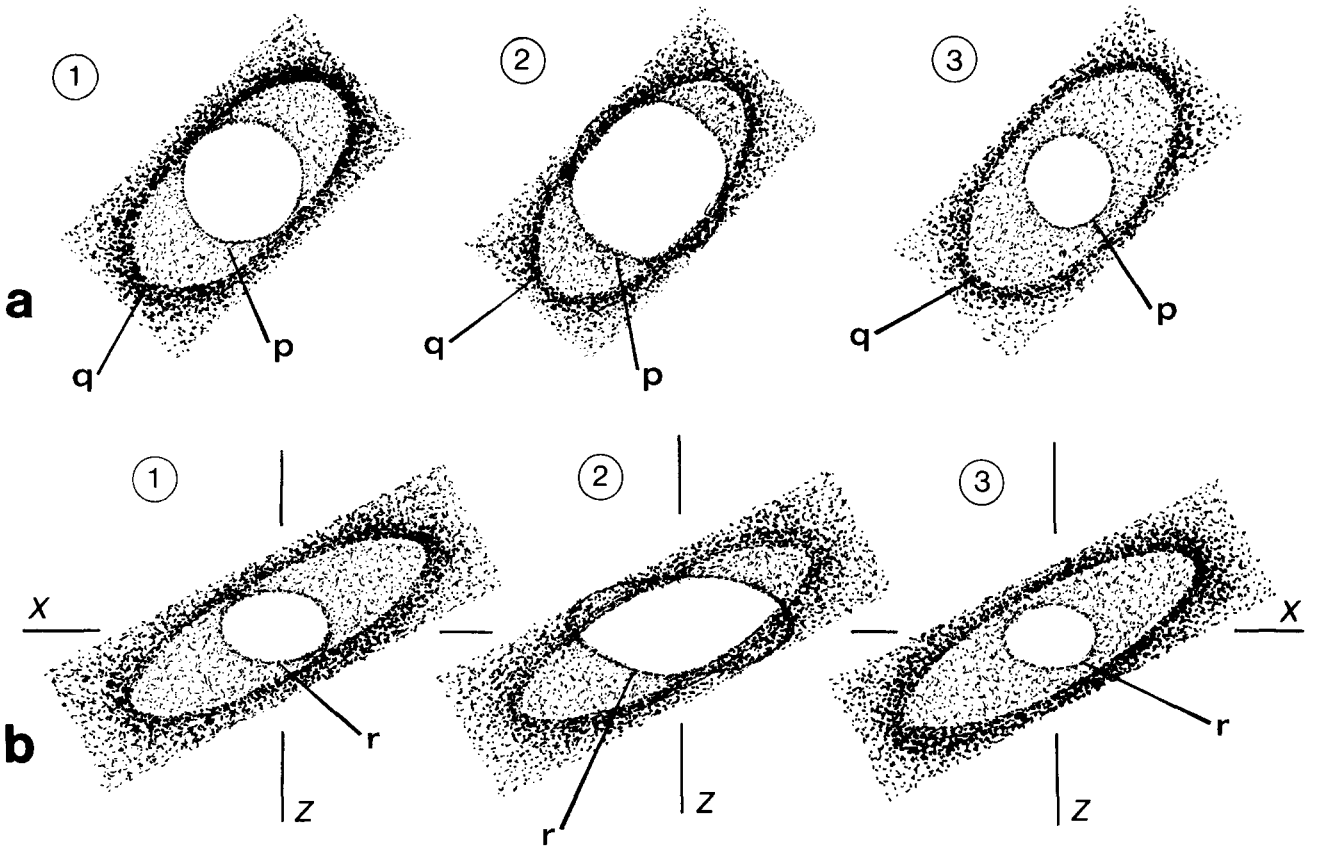


Fig. 7. Types of Fry's diagrams relative to samples including objects in part affected by a sedimentary fabric: models with two shape of markers (see Fig. 6), an elliptical one with a constant axial ratio (called A), an initial circular one (called B). Model 1 (corresponding to figure 6): the diameter of B is equal to the small axis of A. Model 2: the diameter of B is greater than the small axis of A. Model 3: the diameter of B is less than the small axis of A. (a) Fry's diagrams corresponding to the non deformed models: p = circle resulting from the relations between the objects A. q = ellipse, resulting from the relation between the objects B; it represents the sedimentary fabric. (b) Fry's diagrams for the deformed models: The circle is deformed and now represent the strain ellipse (r).

Table 1. Characteristics of measured finite strain ellipsoids: $X/Y$; $Y/Z$: ellipse axial ratios; $(X<Y<Z)$; $\triangle$ = estimated error (due to ellipse resolution on the Fry's diagram); $N^b$ $P^{ts}$: number of points; 'x': no results in this section; $K$ (Flinn 1962) given by $K=(X/Y-1)/(Y/Z-1)$.

| Sample | $X/Y$ | $\triangle$ | $N^b$ $P^{ts}$ | $Y/Z$ | $\triangle$ | $N^b$ $P^{ts}$ | $X/Z$ | $\triangle$ | $N^b$ $P^{ts}$ | $K$ |
|---|---|---|---|---|---|---|---|---|---|---|
| 1 | 2.5 | 0.3 | 87 | 2.5 | 0.3 | 82 | 6.1 | . | x | 0.97 |
| 2 | 2.9 | 0.4 | 113 | 3.0 | 0.4 | 153 | 8.7 | . | x | 0.95 |
| 3 | 3.6 | 0.5 | 167 | 3.6 | 0.6 | 258 | 12.9 | . | x | 1 |
| 4 | 2.3 | 0.5 | 85 | 2.2 | 0.4 | 88 | 4.8 | . | x | 1.1 |
| 5 | 2.2 | 0.3 | x | 1.9 | 0.2 | 275 | 4.2 | 0.2 | 411 | 1.3 |
| 6 | 2.7 | 0.4 | 106 | 2.8 | 0.3 | 86 | 7.8 | . | x | 0.95 |
| 7 | 2.7 | 0.3 | 142 | 2.4 | 0.3 | 164 | 6.6 | . | x | 1.25 |
| 8 | 4.1 | 0.8 | 99 | 2.8 | 0.4 | 153 | 11.2 | . | x | 1.75 |
| 9 | 4.5 | 0.7 | 236 | 2.9 | 0.4 | 206 | 13.0 | . | x | 1.9 |
| 10 | 4.7 | 0.8 | 98 | 3.3 | 0.5 | 85 | 15.5 | . | x | 1.6 |
| 11 | 4.7 | 0.8 | 164 | 3.2 | 0.4 | 234 | 13.0 | 2.0 | 409 | 1.6 |
| 12 | 3.5 | 0.6 | 119 | 2.9 | 0.3 | 139 | 8.0 | 2.5 | 101 | 1.3 |
| 13 | 3.2 | 0.4 | 86 | 3.3 | 0.4 | 130 | 10.5 | . | x | 0.95 |

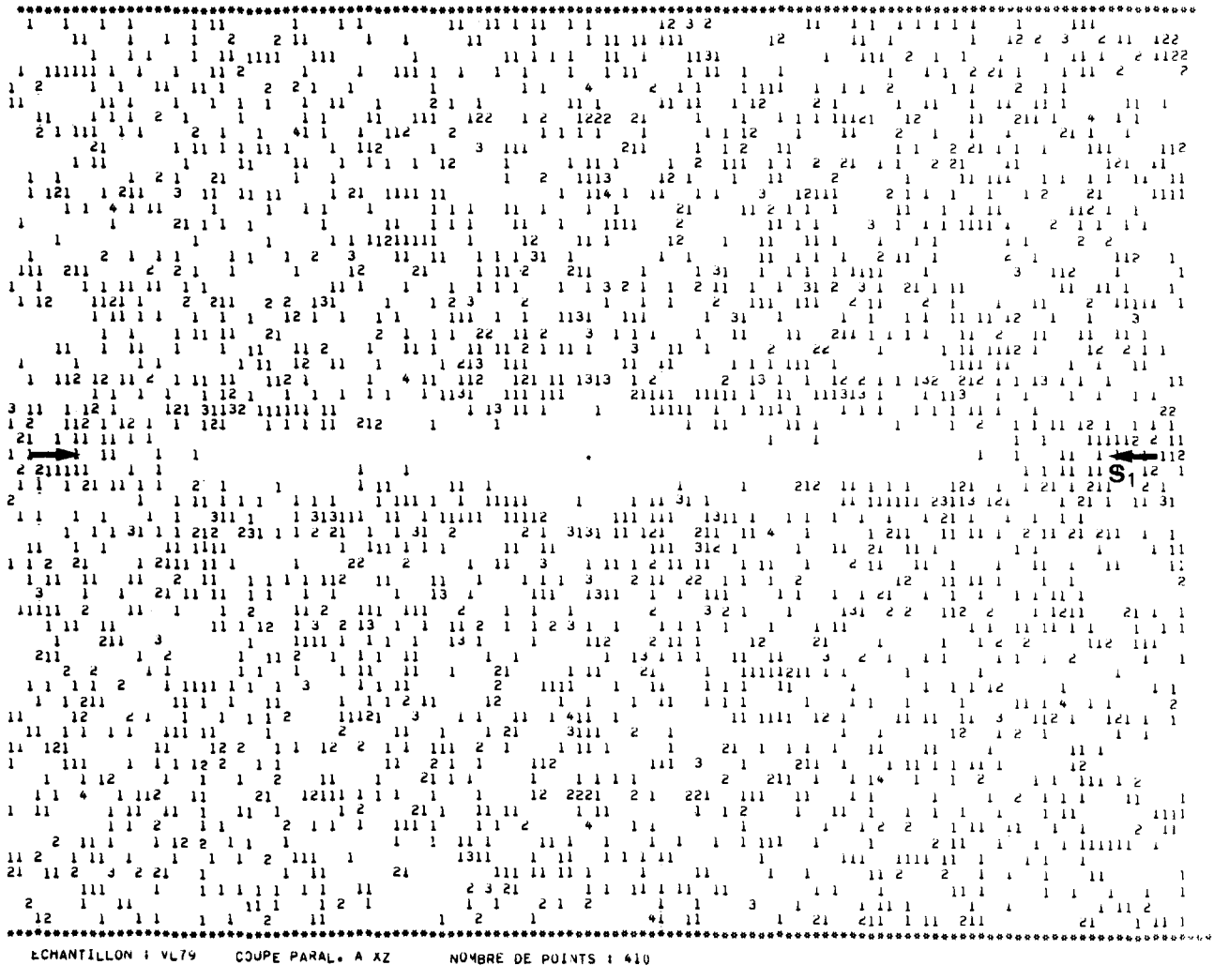


Fig. 8. Example of Fry plot obtained in a section parallel to $XZ$ (sample 11, 409 objects)—$S_1$ is cleavage; $X/Z = 12$.

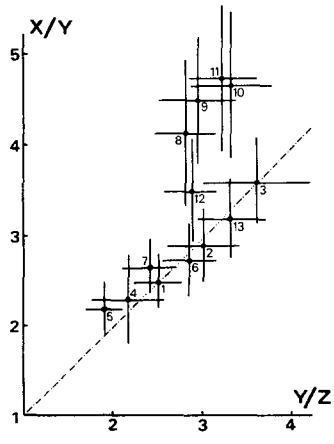


Fig. 9. Measured ellipsoids and errors (see Table 1) plotted on a Flinn diagram.

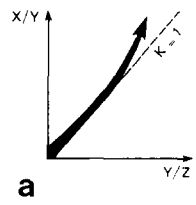


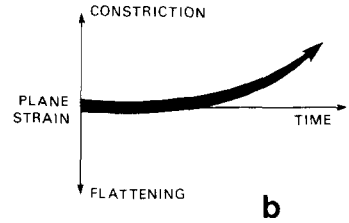


Fig. 10. Proposed strain path, (a) in a Flinn diagram and (b) in a diagram showing the evolution of $K$ during deformation.

(strain path) relates all the points on the Flinn diagram (Figs. 9 & 10(a) and Hobbs *et al.* 1976). This strain path means, for example, that sample 11 had undergone a plane strain (as sample 1) before a late, slightly constrictional, strain (Fig. 10b). As a working hypothesis we propose that the occurrence of this constrictional strain resulted from the mechanics and kinematics of cleavage anisotropy (Brun & Choukroune 1981) and not from external effects.

## CONCLUSIONS

In deep-level tectonites individual crystals are the most abundant pretectonic objects. Taking those objects as markers, we have applied the Fry's method (1979) to the finite-strain determination of the rocks. We show that it may be a very useful technique when the pretectonic objects are well defined and if the number of tectonic clasts is low. According to the section analysed and the strain intensity, a number of points between 100 and 400 is required for a good estimate of the finite strain ellipses. It is possible to determine their axial ratios up to a value of 12. Taking some precautions, the effect of a pretectonic shape fabric (sedimentary) may be neglected in some cases.

We have applied this method to the Cévennes porphyroid gneisses and we propose a strain path according to (a) the macroscopic characters of the deformation, (b) the microtectonic observations and (c) the analysis of quartz fabric. Applied to deep level tectonites, it is obvious that Fry's method also integrates the latest increments of the deformation: the deformation path characterized mainly by plane strain, shows the occurrence of a slightly constrictional deformation at the end of the major tectonic event. Such strain paths seems to be usual in areas deformed under a simple-shear regime, but the mechanism is not well understood. This plane strain pattern is compatible with the deformation of the series of Cévennes gneissic rocks in a shear regime.

*Acknowledgements*—We thank J. P. Burg, A. Etchecopar, P. Laurent and M. Mattauer for reviews of earlier versions of the manuscript.

## REFERENCES

Blacic, J. D. 1975. Plastic deformation mechanisms in quartz: the effects of water. *Tectonophysics* **27**, 271–294.

Bouchez, J. L. 1978. Preferred orientation of quartz c-axes in some tectonites: kinematic inferrences. *Tectonophysics* **49**, T25–T30.

Brouder, P. 1963. Description d'une succession lithologique avec niveaux repères dans les schistes cristallins des Cévennes. *Bull. Soc. géol. Fr.* 7 *Ser.* **5**, 828–834.

Brun, J. P. & Choukroune, P. 1981. Déformation progressive et structures crustales. *Revue Géol. dyn. Géogr. Phys.* **23**, 177–193.

Brunel, M. 1980. Quartz fabric in shear-zone mylonites: evidence for a major imprint due to late strain increments. *Tectonophysics* **64**, T33–T44.

Burg, J. P. 1981. Tectonique tangentielle hercynienne en Vendée littorale: signification des linéations d'étirement E–W dans les porphyroïdes à foliation horizontale. *C.r. hebd. Séanc. Acad. Sci., Paris* **2** T **293**, 849–854.

Burg, J. P. & Matte, Ph. 1978. A cross section through the French Massif Central and the scope of its Variscan geodynamic evolution. *Z. dt. geol. Ges.* **129**, 429–460.

Choukroune, P. 1971. Contribution à l'étude des mécanismes de la déformation avec shistosité grâce aux cristallisations syncinématiques dans les zones abritées. *Bull. Soc. géol. Fr.* 7 *Ser.* **13**, 257–271.

Cloos, F. 1947. Oolite deformation in the South Mountain Fold, Maryland. *Bull. geol. Soc. Am.* **58**, 843–918.

Etchecopar, A. 1977. Kinematic model of progressive deformation in polycristalline aggregate. *Tectonophysics* **39**, 121–139.

Flinn, D. 1962. On folding during three dimensional progressive deformation. *Q. Jl geol. Soc.* **118**, 385–433.

Flinn, D. 1965. On the symmetry principle and the deformation ellipsoid. *Geol. Mag.* **102**, 36–45.

Fry, N. 1979. Random point distributions and strain measurement in rocks. *Tectonophysics* **60**, 89–105.

Gratier, J. P. & Vialon, P. 1980. Deformation pattern in a heterogeneous material: folded and cleaved sedimentary cover immediately overlying a cristalline basement (Oisans – French Alps). *Tectonophysics* **65**, 151–180.

Hanmer, S. K. 1979. The role of discrete heterogeneities and linear fabrics in the formation of crenulations. *J. Struct. Geol.* **1**, 81–91.

Hanna, S. S. & Fry, N. 1979. A comparison of methods of strain determination in rocks from south west Dyfed (Pembrokeshire) and adjacent areas. *J. Struct. Geol.* **1**, 155–162.

Henderson, J. R. 1981. Structural analysis of sheath folds with horizontal X-axes, NE Canada. *J. Struct. Geol.* **3**, 203–210.

Hobbs, B., Means, W. & Williams, P. 1976. *An Outline of Structural Geology*. Wiley, New York.

Hugon, H. & Le Corre, C. 1979. Mise en évidence d'une déformation hercynienne en régime cisaillant progressif dans le Massif cambrien de Rocroi. *C. r. hebd. Séanc. Acad. Sci., Paris* **D 280**, 615–618.

Laurent, P. & Etchecopar, A. 1976. Mise en évidence à l'aide de la fabrique du quartz d'un cisaillement simple à déversement W dans le Massif de Dora-Maira (Alpes). *Bull. Soc. geol. Fr.*, 7 *Ser.* **18**, 1387–1393.

Lister, G. S., Paterson, M. S. & Hobbs, B. E. 1978. The simulation of fabric development in plastic deformation and its application to quartzite: the model. *Tectonophysics* **45**, 107–158.

Lister, G. S. & Price, G. P. 1978. Fabric development in quartz feldspar mylonite. *Tectonophysics* **49**, 37–78.

Lister, G. S. & Williams, P. E. 1979. Fabric development in shear zones: theoretical controls and observed phenomena. *J. Struct. Geol.* **1**, 283–297.

Lister, G. S. & Hobbs, B. E. 1980. The simulation of fabric development during plastic deformation and its application to quartzites: the influence of deformation history. *J. Struct. Geol.* **2**, 355–370.

Mattauer, M. & Etchecopar, A. 1976. Arguments en faveur de chevauchements du type himmalayen dans la chaîne hercynienne du Massif Central français. *Coll. Int. CNRS* **268**, 261–267.

Nicolas, A. & Poirier, J. P. 1976. *Crystalline Plasticity and Solid State Flow in Metamorphic Rocks*. Wiley, London.

Pellet, J. 1972. Données lithologiques et structurales sur le terrains cristallins cévenols affectés par l'accident de Villefort. *Bull. Serv. Carte. geol. Fr.* **282T**, 61.

Ramsay, J. G. 1967. *Folding and Fracturing of Rocks*. McGraw-Hill, New York.

Ramsay, J. G. 1976. Displacement and strain. *Phil. Trans. R. Soc.* **A283**, 3–25.

Roger, G. 1969. Etude géologique de la Cézarenque et du SE du Mont Lozère (France). *Mém. Bur. Rech. géol. min. Fr.* **66**.

Shuaib, S. M. 1952. Géologie de la partie méridionale des Cévennes dans le Massif Central français. Unpublished thesis, Clermont-Ferrand.

Steck, A. 1980. Deux directions principales du flux synmétamorphique dans les alpes centrales. *Bull. Soc. Vaud. Sci. Nat.* **358**, **75**, 141–149.

Tullis, J., Christie, J. M. & Griggs, D. T. 1973. Microstructures and preferred orientations of experimentally deformed quartz. *Bull. geol. Soc. Am.* **84**, 297–314.

Turner, F. J. & Weiss, L. E. 1963. *Structural Analysis of Metamorphic Tectonites*. McGraw-Hill, New York.

White, S. 1976. The effect of strain on the microstructures, fabrics and deformation mechanisms in quartz. *Phil. Trans. R. Soc.* **A283**, 69–86.